Electromagnetic-Wave Excitation in a Large Laboratory Beam-Plasma System

D. A. Whelan and R. L. Stenzel
Department of Physics, University of California, Los Angeles, California 90024
(Received 3 June 1981)

Electromagnetic radiation is observed when an electron beam is injected into a uniform quiescent magnetoplasma. The emission peaks near the electron plasma frequency ($\omega \gtrsim \omega_p \gg \omega_c$) and is found to result from the scattering of unstable intense electrostatic plasma waves off self-consistently produced ion acoustic waves with wave vectors $k_i \simeq k_e$. The emission is localized, polarized, and negligible in intensity at $\omega = 2\omega_{pe}$. Space-time growth and ω-k properties of the three-wave interaction are presented.

PACS numbers: 52.35.Hr, 52.25.Ps, 52.35.Mw, 96.60.Tf

The mechanism by which unstable electrostatic waves of a beam-plasma system are converted into observed electromagnetic waves is of current interest in space physics (kilometer radiation,[1] type-III solar burst,[2] and artificial beam injections[3]) and in tokamak fusion research.[4] The simplest process, i.e., conversion of electrostatic to electromagnetic waves at the critical layer ($\omega = \omega_p$), is well understood in both theory[5] and experiment[6] but cannot explain the radiation from uniform plasmas. There, the scattering of electron plasma waves off ion acoustic modes and other electron plasma waves has been theoretically shown to produce electromagnetic waves near $\omega \gtrsim \omega_{pe}$ and $2\omega_{pe}$, respectively.[7]

In spite of considerable effort in theory and simulation of the nonlinear instability (soliton collapse[8]) the experimental observations have not yet clearly established these emission processes. This is partly due to unavoidable density gradients in small laboratory devices[9] and partly due to diagnostic difficulties in space[10] and high-temperature plasmas.[11] In the present work these difficulties are overcome with use of a large laboratory plasma in a parameter range suitable for detailed diagnostics. A finite-diameter electron beam is injected into a uniform quiescent afterglow plasma of dimensions large compared with electromagnetic wavelengths. Electrostatic waves grow and decay within the uniform plasma volume so that linear mode conversion can be excluded. Waves and particles are diagnosed *in situ* with probes offering time and space resolution for the pulsed beam-plasma interaction. The observations indicate that upon beam injection electron plasma waves ($\omega \gtrsim \omega_p$) rapidly grow and saturate, temporally within $t \simeq 10^4 \omega_{pe}^{-1} \simeq 0.2$ μsec, spatially within $z \simeq 60 k_\parallel^{-1} \simeq 2$ cm. Then, on a slower time scale ($t \simeq 10^2 \omega_{pi}^{-1} \simeq 2$ μsec in Xe), ion density fluctuations grow and saturate. Electromagnetic emission is observed to grow at the *same* slow rate as the density fluctuations showing conclusively that the generation mechanism involves a three-wave interaction. With use of correlation techniques, the wave vectors of both high-frequency (~6 GHz) and low-frequency (~2 MHz) electrostatic modes have been measured. These observations confirm the decay of unstable electron plasma waves (ω_e, k_e) into electromagnetic waves (ω_0, k_0) and ion acoustic modes (ω_i, k_i), i.e., $\omega_e = \omega_0 + \omega_i$, $k_e = k_i + k_0 \simeq k_i$.

The experimental setup is shown in Fig. 1. A pulsed magnetized discharge plasma is produced with a 1-m-diam oxide-coated cathode and the experiment is performed in the quiescent afterglow of typical parameters $n_e \simeq 5 \times 10^{11}$ cm^{-3}, $T_e \simeq 10 T_i \simeq 3$ eV, $B_0 \simeq 20$ G, and pressures of 2×10^{-4} Torr in H_2, He, Ar, and Xe. A pulsed electron beam ($V_b \simeq 500$ V, $I_b \lesssim 1$ A, $n_b/n_0 \lesssim 1\%$, rise time $\lesssim 100$ nsec) is injected from a small oxide cathode (0.8 cm diam) along the axis of the 2-m-long plasma at various pitch angles ($0 < \theta_b < 360°$). Plasma properties are derived from Langmuir probes and test wave measurements. The electromagnetic radiation is received either

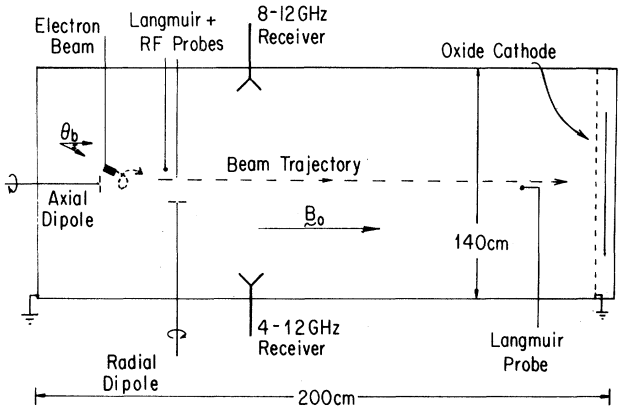

FIG. 1. Schematic diagram of the experimental setup.

with fixed horn antennas outside the plasma column or with moveable dipole antennas inside the plasma. Coaxial rf probes (0.1 mm diam, 1 mm length) are used to detect electrostatic high- and low-frequency modes. The microwave receiver consists of a broadband mixer, local oscillator, i.f. amplifier, crystal detector, and fast oscilloscope with an overall noise figure $F \simeq 8$ dB and temporal resolution $\Delta t \simeq 10$ nsec. Cross-correlation measurements are performed with two identical probes and receivers.

We start the presentation of experimental results with the electron plasma waves which are the primary mode in a beam-plasma instability. Figure 2(a) shows the relative wave intensity along the beam as determined with a broadband square-law detector. The cross-correlation function shown under the envelope exhibits short wavelength ($\lambda_{\parallel} \approx 2$ mm) and a correlation length $L_c \lesssim 1$ cm. Instead of the passive noise analysis, we have also excited test electron plasma waves; a typical interferometer trace is also shown. Test waves growing along the beam can be excited in the same frequency range as the natural emission. These phase-resolved wave and correlation measurements in the GHz regime require extreme care and have, to our knowledge, not been reported before. The dispersion of the test waves and of the dominant spontaneous mode, displayed in Fig. 2(b), clearly identifies them as electron plasma waves. The initial spatial growth rate shown in Fig. 2(c) scales with beam density like $(n_b/n_e)^{1/3}$ as expected for cold beam injection. For $z > 2$ cm the beam distribution is broadened which saturates the instability and finally leads to wave decay when the convective loss exceeds the reduced growth rate. The intense plasma waves are confined to a relatively small volume ($\Delta r \sim 1$ cm, $\Delta z \sim 2$ cm) in comparison with which the plasma is uniform and unbounded.

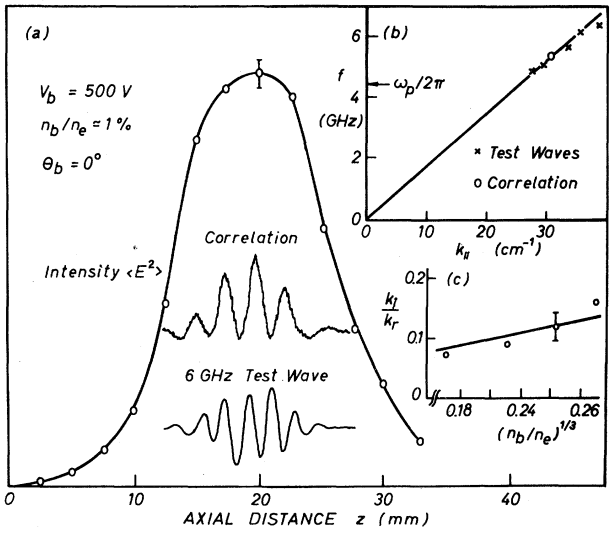

FIG. 2. (a) Relative wave intensity $\langle E^2 \rangle$ of the electrostatic high-frequency mode vs distance along the beam. Insets show cross-correlation function $\langle E_1 E_2 \rangle$ and test wave $E\cos kz$. (b) Dispersion $\omega(k)$ identifies the electrostatic mode as electron plasma waves propagating with the beam ($\omega = kv_b$) just above the electron plasma frequency ω_p. (c) Initial spatial growth rate k_i/k_r scales with beam density [$\propto (n_b/n_e)^{1/3}$] as expected for cold beam injection.

Besides the high-frequency electrostatic waves, beam injection also gives rise to strong ($\delta n_i/n_i \simeq 6\%$) low-frequency density fluctuations whose properties are summarized in Fig. 3. Figure 3(a) shows the fluctuations in the electron saturation current for a single beam pulse which are recorded digitally with an 8-bit, 20-MHz analog-to-digital converter. A fast Fourier transform obtained on-line with an array processor is shown in Fig. 3(b). Waveform and spectra exhibit a dominant mode at $f \simeq 1.5$ MHz. With increasing beam density the width of the low-frequency spectrum broadens. Using tuned filters we perform cross-power spectral density measurements, an example of which is shown in the inset in Fig. 3(c). From such measurements we conclude that the low-frequency noise exhibits the dispersion of ion acoustic waves. Moreover, from phase-delay measurements we establish that the sound waves propagate in the beam direction. Thus, the dominant ion sound mode has a wave vector $k_i \simeq 31$ cm^{-1} which closely matches that of the unstable electron plasma waves.

Electromagnetic radiation from the beam-plasma system is observed with microwave antennas outside the plasma (all probes removed) or with coaxial-probe dipoles which can be moved radially through the plasma for purpose of wavelength and polarization measurements. The frequency spectrum obtained from a fast sweep of the local oscillator during a single beam pulse is a few percent wide and centered slightly above the plasma frequency. The second harmonic emission is much weaker than the fundamental one, $P(2\omega_p) \simeq P(\omega_p) - 30$ dB where $P(\omega_p) \approx 10^{-3}$ W. Measurements of the wavelength, $\lambda_0 = (c/f)(1 - \omega_p^2/\omega^2)^{-1/2} \gtrsim 10$ cm, confirm that the emission is electromagnetic and yield an independent calibration for the electron density. From the rotation of orthogonal dipoles, the polarization of the electric

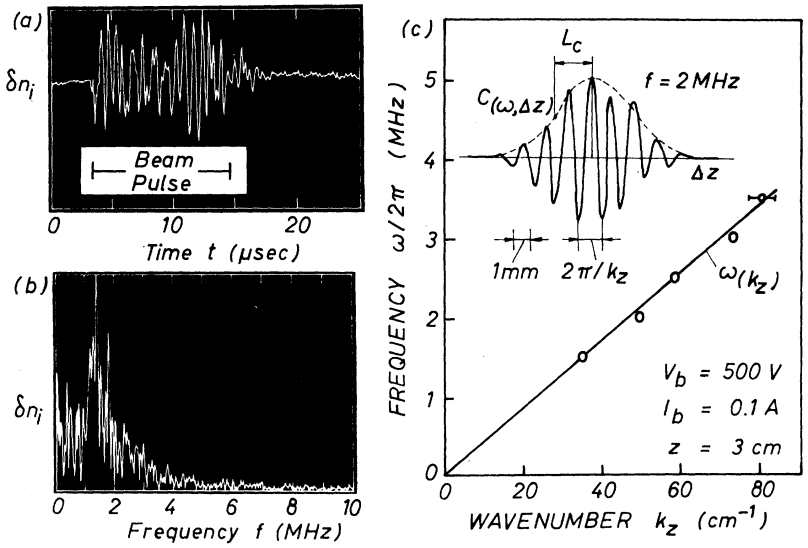

FIG. 3. (a) Low-frequency density fluctuations $\delta n_i(t)$ generated during beam injection. (b) Fast Fourier transform exhibits dominant low-frequency mode at $f \simeq 1.5$ MHz. (c) Fluctuation analysis by measuring cross-power spectral densities (see inset) shows the dispersion of ion sound waves ($kT_e \simeq 3$ eV, Ar). Dominant mode has the same wave vector $k_\parallel \simeq 31$ cm^{-1} as electron plasma waves.

field near but outside the beam is found to be $\vec{E} \parallel \vec{v}_b$. By scanning the dipoles through the plasma, the source region for the electromagnetic emission is found to lie within the first few centimeters from the beam injection point where the electrostatic wave amplitudes peak.

The proposed generation mechanism of the electromagnetic waves is conclusively confirmed by observing the temporal evolution of the instability

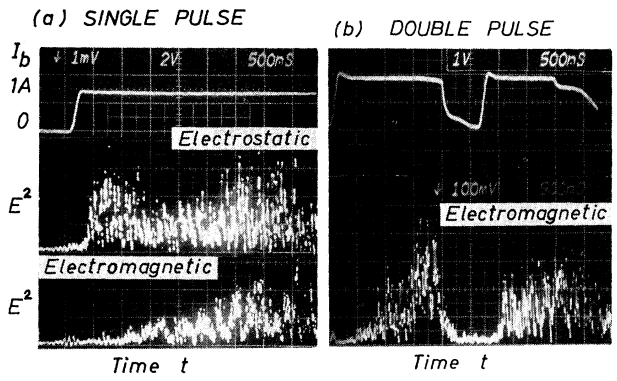

FIG. 4. Temporal growth of electromagnetic waves and plasma waves for (a) single and (b) double beam current pulses I_b. The electromagnetic emission grows on the slow time scale of ion acoustic waves [(a) $\Delta t_i \simeq 2$ μsec, Xe]. If an initial sound wave is present, as for the second pulse in (b), the electromagnetic emission rises as fast as the electrostatic one [(b) Ar, $V_b = 400$ V, $f \simeq 5.5$ GHz].

summarized in Fig. 4. Upon turn on of the beam current [Fig. 4(a), top trace] electrostatic plasma waves grow and saturate within $\Delta t_e \simeq 200$ nsec while the electromagnetic waves grow slowly on the same time scale Δt_i as the ion acoustic waves. This time scale increases systematically with ion mass as verified by operating with H_2^+, He^+, Ar^+, and Xe^+ [Fig. 4(a), $\Delta t_i \simeq 2$ μsec]. However, if an initial turbulence level is present the electromagnetic emission grows as fast as the electrostatic one. This is demonstrated in Fig. 4(b), where two consecutive beam pulses are injected. The density fluctuations produced during the first pulse are still present when the second pulse is injected [see decay in Fig. 3(a)] so that mode coupling takes place immediately.

Thus, both the time evolution and the ω-k measurements demonstrate experimentally how the observed electromagnetic emission is generated in a uniform beam-plasma system. Quantitatively, this radiation mechanism has been treated by Dawson.[12] The radiated power due to electrostatic waves of intensity $\epsilon_L(\omega)$ scattering off thermal ion fluctuations is given by $P = \int P_\omega \, d\omega = \frac{1}{3} e^2(\omega_p/m_e c^3) \times \int (\omega^2 - \omega_p^2)^{1/2} \epsilon_L(\omega) d\omega$. For nonthermal fluctuations (ion waves) this value is enhanced by a factor $\beta = (4\pi)^{-1}(\delta n_i/n_i)(k/\Delta k) n_i \lambda_e^3$. For our parameters ($\delta n_i/n_i \simeq 3\%$, $\Delta k/k \simeq 20\%$, $\lambda_e \simeq 2$ mm, $\int \epsilon_L(\omega) d\omega \simeq 0.1 nkT \simeq 2.5 \times 10^{-8}$ J cm^{-3}) we find for a radiating volume of ~2 cm^3 a total power $P \simeq 1.5$

mW in good agreement with the observed value.

The authors acknowledge helpful discussions with Dr. G. Morales, Dr. J. Dawson, and Dr. B. Fried, and help with the digital data processing from Dr. W. Gekelman. This work was supported by the National Aeronautics and Space Administration under Grants No. NSF-7616 and No. NAGW-180.

[1]J. E. Maggs, J. Geomagn. Geoelectr. 30, 273 (1978).
[2]K. Papadopoulos, Rev. Geophys. Space Phys. 17, 624 (1979).
[3]J. Lavergnat *et al.*, Ann. Geophys. 36, 323 (1980).
[4]I. H. Hutchinson and S. E. Kissel, Phys. Fluids 23, 1698 (1980).
[5]A. D. Piliya, Zh. Tekh. Fiz. 36, 819 (1966) [Sov. Phys. Tech. Phys. 11, 609 (1966)].
[6]R. L. Stenzel, A. Y. Wong, and H. C. Kim, Phys. Rev. Lett. 32, 654 (1974).
[7]V. N. Tsytovich, *Theory of Turbulent Plasma* (Consultants Bureau, New York, 1977), p. 350; D. B. Melrose, Space Science Rev. 26, 3 (1980).
[8]V. E. Zakharov, A. F. Mastryukov, and S. V. Synakh, Fiz. Plazmy 1, 614 (1975) [Sov. J. Plasma Phys. 1, 339 (1975)]; K. Papadopoulos and H. P. Freund, Geophys. Res. Lett. 5, 881 (1978); M. V. Goldman, G. F. Reiter, and D. R. Nicholson, Phys. Fluids 23, 388 (1980).
[9]L. D. Bollinger and H. Böhmer, Phys. Rev. Lett. 26, 535 (1971).
[10]G. Benford *et al.*, Phys. Rev. Lett. 45, 1182 (1980).
[11]D. A. Gurnett and R. R. Anderson, Science 194, 1159 (1976).
[12]J. M. Dawson, *Advances in Plasma Physics*, edited by A. Simon and W. B. Thompson (Wiley, New York, 1968), Vol. 1.

Nonlinear Penetration of Upper-Hybrid Waves Induced by Parametric Instabilities of a Plasma in an Inhomogeneous Magnetic Field

A. T. Lin and Chih-Chien Lin
Department of Physics, University of California at Los Angeles, Los Angeles, California 90024
(Received 3 April 1981)

It is observed that with a sufficiently large incident extraordinary wave amplitude, the electrostatic upper hybrid wave resulting from the mode conversion process at the resonant layer can scatter off the lower hybrid wave and penetrate through its original cutoff to a distance proportional to the product of the scale length and the square root of the mass ratio. A substantial number of energetic ions also appear in the resonant region which is well inside the plasma slab as a result of lower hybrid wave excitation.

PACS numbers: 52.35.-g

The availability of high power Gyrotrons[1] and the promise of even higher power tunable microwave sources from free-electron lasers[2] have attracted a great deal of attention to electron heating in a magnetized plasma.[3-5] In addition to the ultimate heating of plasma to fusion temperature, electron heating at frequencies around cyclotron range could enhance the stability of an Elmo Bumpy Torus by creating high-β electron annulus,[6] provide a thermal barrier for mirror devices,[7] and modify the plasma profile to improve stability. The heating mechanisms are mainly due to cyclotron resonant heating and upper hybrid mode conversion.[8] In the latter case, the electrostatic field at the resonant layer can attain a very large value limited only by dissipation and thermal convection. This large amplitude electrostatic oscillation is capable of giving rise to a variety of nonlinear effects. In this Letter, the parametric decay process and its enhancement of wave penetration through the original cutoff are investigated by use of computer simulations. To the best of our knowledge, this is the first time that a highly localized parametric decay instability has been observed in computer simulations for a strongly magnetized plasma situated in an inhomogenous magnetic field.

As an extraordinary wave of given ω_0 propagates to the upper hybrid resonant layer, both its phase velocity and group velocity approach zero in a collisionless cold plasma ($T_e \ll mc^2$), and the wave energy is converted into upper hybrid oscillations. This mode conversion process will be investigated in a simple configuration. Consider a normal-incident [$\vec{k} = k(x)\hat{x}$] extraordinary wave which propagates from the high-field side [$\vec{B}_0 = B_0(x)\hat{z}$] in a plasma with uniform density. The magnetic field is assumed to vary linearly

$$B_0(x)/B_0(0) = 1 - x/L_m , \quad (1)$$

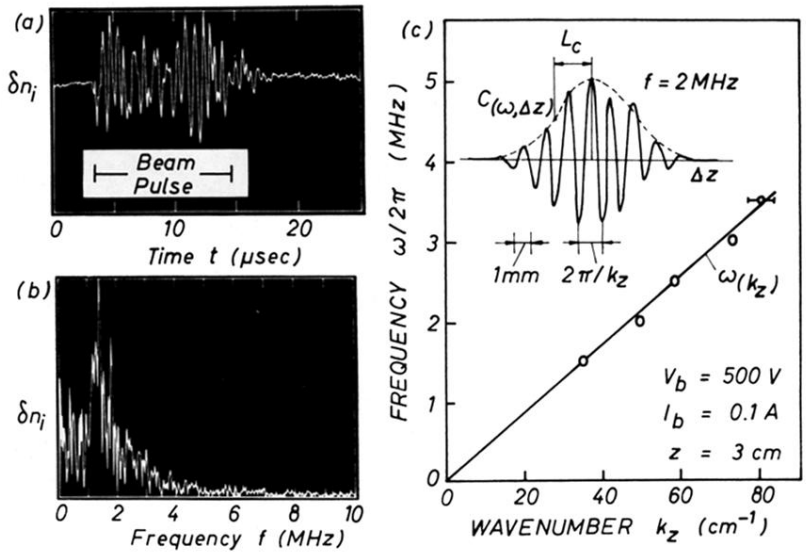

FIG. 3. (a) Low-frequency density fluctuations $\delta n_i(t)$ generated during beam injection. (b) Fast Fourier transform exhibits dominant low-frequency mode at $f \simeq 1.5$ MHz. (c) Fluctuation analysis by measuring cross-power spectral densities (see inset) shows the dispersion of ion sound waves ($kT_e \simeq 3$ eV, Ar). Dominant mode has the same wave vector $k_\parallel \simeq 31$ cm^{-1} as electron plasma waves.

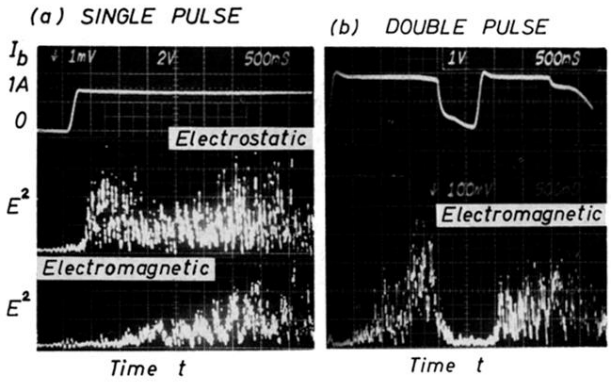

FIG. 4. Temporal growth of electromagnetic waves and plasma waves for (a) single and (b) double beam current pulses I_b. The electromagnetic emission grows on the slow time scale of ion acoustic waves [(a) $\Delta t_i \simeq 2$ μsec, Xe]. If an initial sound wave is present, as for the second pulse in (b), the electromagnetic emission rises as fast as the electrostatic one [(b) Ar, $V_b = 400$ V, $f \simeq 5.5$ GHz].